Kenji Kamimura*, Koji Kimura, Shinya Hosokawa,
Naohisa Happo, Hiroyuki Ikemoto, Yuji Sutou, Satoshi Shindo,
Yuta Saito, and Junichi Koike

XAFS Analysis of Crystal $GeCu_2Te_3$ Phase Change Material

DOI 10.1515/zpch-2015-0672
Received July 30, 2015; accepted October 13, 2015

Abstract: The structure of crystal $GeCu_2Te_3$ was investigated by X-ray absorption fine structure (XAFS) measurement. We found that the Ge–Te interatomic distances obtained from XAFS are larger than those obtained from X-ray diffraction, and the Cu–Te distances are smaller. The averaged Ge–Te and Cu–Te distances obtained from XAFS are almost equal to the corresponding interatomic distances in amorphous $GeCu_2Te_3$. Therefore both crystal and amorphous $GeCu_2Te_3$ seem to be built up of the same local configurations of $GeTe_4$ and $CuTe_4$ tetrahedrons. This would be the reason why the phase change in $GeCu_2Te_3$ occurs very fast.

Keywords: Phase Change Material, XAFS.

1 Introduction

$Ge_2Sb_2Te_5$ has intensively been studied for the use of phase change random access memory (PCRAM) because of its fast phase-change speed and good reversibility between amorphous and crystalline states [1]. PCRAM is operated by Joule heating to induce a phase transition between a high-resistance amorphous phase

***Corresponding author: Kenji Kamimura,** Department of Physics, Graduate School of Science and Technology, Kumamoto University, Kumamoto, 860-8555, Japan, e-mail: 148d8003@st.kumamoto-u.ac.jp
Koji Kimura, Shinya Hosokawa: Department of Physics, Graduate School of Science and Technology, Kumamoto University, Kumamoto, 860-8555, Japan
Naohisa Happo: Graduate School of Information Sciences, Hiroshima City University, Hiroshima 731-3194, Japan
Hiroyuki Ikemoto: Department of Physics, Faculty of Science, University of Toyama, Toyama 930-8555, Japan
Yuji Sutou, Satoshi Shindo, Yuta Saito, Junichi Koike: Department of Materials Science, Graduate School of Engineering, Tohoku University, Sendai, 980-8579, Japan

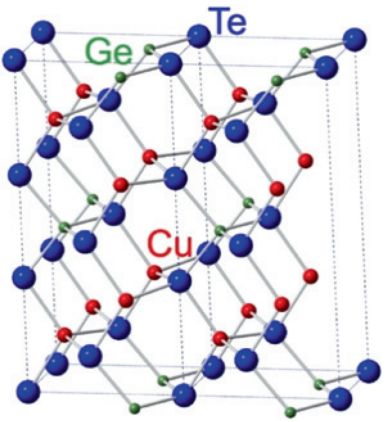

Figure 1: Crystal structure of $GeCu_2Te_3$ determined by XRD [3].

(reset state) and a crystalline phase with a low resistance (set state) of a phase change material [1]. The melting point of typical PCRAM material $Ge_2Sb_2Te_5$ is over 600 °C, which means that a high power consumption is required for its reset operation, while its crystallization temperature is about 150 °C, which limits its data retention capability [1]. Therefore a higher crystallization temperature and a lower melting point are necessary.

The crystallization temperature of $GeCu_2Te_3$ is about 250 °C, while its melting point is around 500 °C [2]. The phase change of $GeCu_2Te_3$ rapidly occurs in about several 10 ns. Therefore $GeCu_2Te_3$ is a promising phase change material with its low power consumption, excellent data retention and high-speed rewriting operation [1]. For the understandings of the fast phase change mechanism between the amorphous and crystalline phases of $GeCu_2Te_3$, it is important to know the local structure of both the phases. X-ray absorption fine structure (XAFS) measurement is excellent method to investigate local structures, and shows distances, coordination numbers, and elements around a selected atom.

Figure 1 shows the structure of crystalline $GeCu_2Te_3$ obtained by X-ray diffraction (XRD) [3]. The crystal has a Cu_2GeSe_3-type orthorhombic structure with a space group of *Imm2* [3]. Another XRD result shows a different space group of tetragonal $CuFeS_2$-type with a space group of *I-42d* [4]. In both the structures, crystalline $GeCu_2Te_3$ is built up of corner-sharing $GeTe_4$ and $CuTe_4$ tetrahedrons.

To investigate the structure of crystalline $GeCu_2Te_3$, we selected XAFS measurement. In this paper, we report our results of XAFS analysis of crystalline $GeCu_2Te_3$ to examine local structures around each element whether the XRD result properly describes the local structures of the $GeCu_2Te_3$ crystal or not.

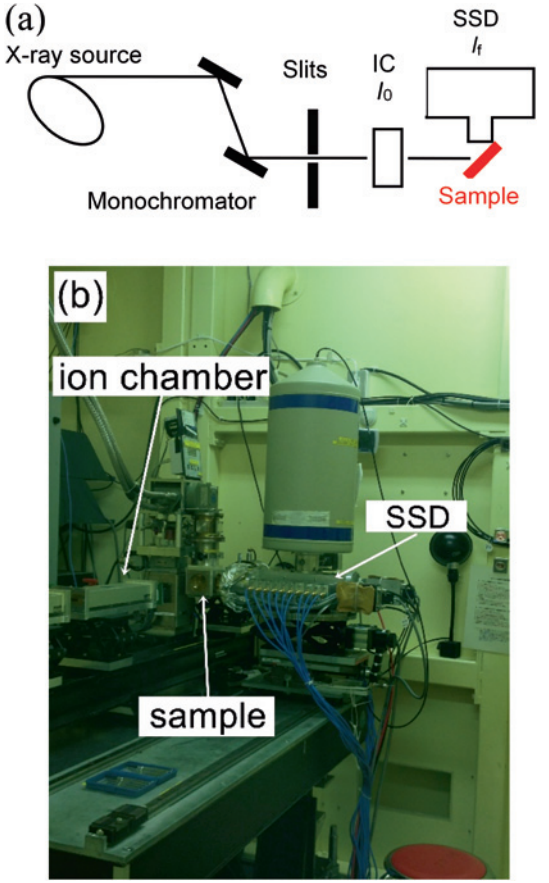

Figure 2: (a) Schematic diagram and (b) photograph of experimental set up used for the present fluorescent XAFS measurement.

2 Experiment and analysis

Amorphous $GeCu_2Te_3$ samples with a thickness of 200 nm were deposited on SiO_2(20 nm)/Si substrates at room temperature by radio-frequency sputtering of a $GeCu_2Te_3$ polycrystalline alloy target [1]. The base pressure of vacuum chamber used for the sample preparation was below 4×10^{-5} Pa and the radio-frequency power for sputtering was 70 W [1]. Then, crystalline $GeCu_2Te_3$ sample was obtained by annealing the amorphous sample at 250 °C. This crystallinity of the $GeCu_2Te_3$ sample was confirmed by XRD.

The XAFS experiment was carried out at BL12C in Photon Factory at High Energy Accelerator Research Organization (PF-KEK). XAFS data were measured in fluorescence mode at 30 K. Figure 2 shows (a) a schematic view and (b) its pho-

tograph of the experimental set up used for the present fluorescent XAFS measurement. X-rays emitting from a bending magnet source are monochromatized by a double Si (111) crystal. The incident X-ray intensity I_0 was measured by an ion chamber (IC). The fluorescent X-ray intensity from the sample I_f was detected by a 19-channels pure Ge solid-state-detector (SSD). XAFS measures the energy dependence of the X-ray absorption coefficient $\mu(E)$ near an absorption edge of a selected element.

$$\mu(E) \propto I_f/I_0. \tag{1}$$

The resulting XAFS function was refined using the path expansion formalism as implemented in the *Artemis* software package [5], based on *Ifeffit* and *FEFF6* [6]. The XRD data of the Cu_2GeSe_3-type structure shown in Figure 1 was selected as an initial condition of the fitting to obtain the interatomic distances.

A Fourier transform-like analysis was carried out for the XAFS oscillations extracted from the raw data. Then, the XAFS oscillations concerning the nearest neighbors were obtained by inverse-Fourier transforms of the nearest neighbor area in the above Fourier transforms. Using theoretical formula of XAFS oscillations, fits are performed, where the theoretical formula is expressed as

$$\chi(k) = S_0^2 \sum_i \frac{N_i}{kR_i^2} F_i(k) \sin(2kR_i + \varphi_i(k)) \exp\left(-2\sigma_i^2 k^2\right). \tag{2}$$

Here S_0^2 is an amplitude reduction factor, N_i coordination numbers of neighboring atoms, R_i nearest neighbor distances, $F_i(k)$ backscattering factors, $\varphi_i(k)$ phase shifts, and σ_i Debye–Waller factors. Since $F_i(k)$ and $\varphi_i(k)$ depend on atomic numbers Z of the scattering atoms, we can also determine the elements of the neighboring atom.

3 Results and discussion

Figure 3 shows $\mu(E)$ near the (a) Ge (11.104 keV) and (b) Cu (8.979 keV) K-edges in crystal $GeCu_2Te_3$. Clear XAFS oscillations are observed near both of the absorption edges.

Figure 4 shows the XAFS oscillations extracted from the raw data near the (a) Ge and (b) Cu K edges. As shown in the figure, the amplitudes of these oscillations have two peaks at about 4.0 Å and 11.0 Å. The existence of these two peaks is characteristic for the heavy elements. This $GeCu_2Te_3$ sample consists Ge, Cu and Te. So the features of these oscillations clearly indicate that the neighboring atoms are mainly composed of Te atoms.

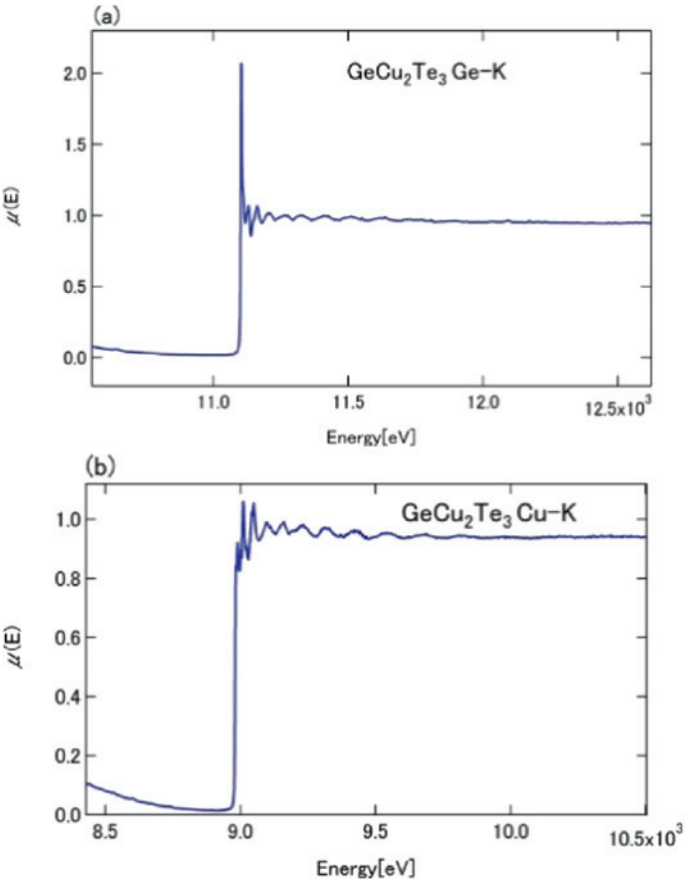

Figure 3: The $\mu(E)$ data near the (a) Ge and (b) Cu K-edges in crystal $GeCu_2Te_3$.

Figures 5 and 6 show (a) the Fourier transforms of XAFS oscillations near the Ge and Cu K edge, respectively, and (b) their inverse-Fourier transforms. The existence of the second peaks at about 3.8 Å suggests that this $GeCu_2Te_3$ sample is not amorphous but crystalline.

Circles and solid lines indicate the experimental data and the best fits of the theory. The thin straight lines show the window function in the R range of 1.57–2.97 Å (Figure 5) and 1.601–3.051 Å (Figure 6) used for the inverse Fourier transforms. We refined only the first peaks in the XAFS data, because the second neighbor signals are much lower than the first peaks. The fit curves coincide well with the experimental data. Fourier transforms of $k^2\chi(k)$ in Figures 5(a) and 6(a) have two peaks due to the shape of backscattering amplitude of Te.

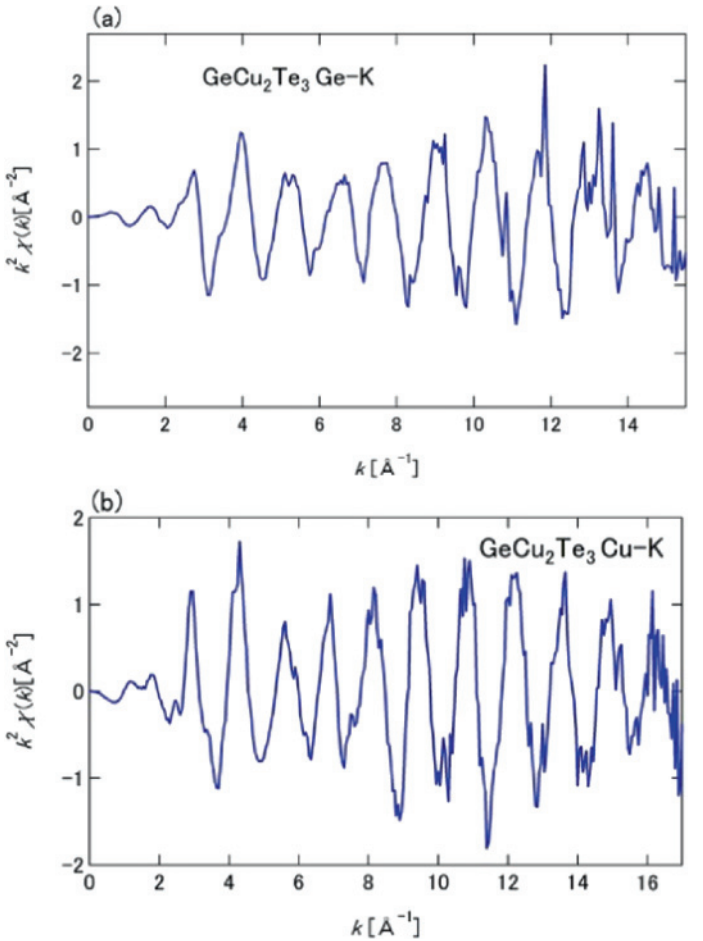

Figure 4: XAFS oscillations extracted from the raw data near the (a) Ge and (b) Cu K edges.

Table 1 shows the coordination numbers N_j, the nearest neighbor distances R_j, and the Debye–Waller factors σ_i^2 in crystal $GeCu_2Te_3$ obtained by the present XAFS analysis. In the crystal $GeCu_2Te_3$, there are two Te sites around Ge and three Te sites around Cu, which have different R_j values. The Ge–Te1 and -Te2 coordination numbers are fixed to be 2 each during the fitting procedure. Then, the obtained distances for Ge–Te1 and -Te2 are 2.585 and 2.617 Å, respectively.

In the same way, the Cu–Te1, -Te2, and -Te3 coordination numbers are fixed to be 2, 1, and 1, respectively, during the fitting procedure. Then, the obtained distances for Cu–Te1, -Te2, and -Te3 are 2.537, 2.574, and 2.531 Å, respectively.

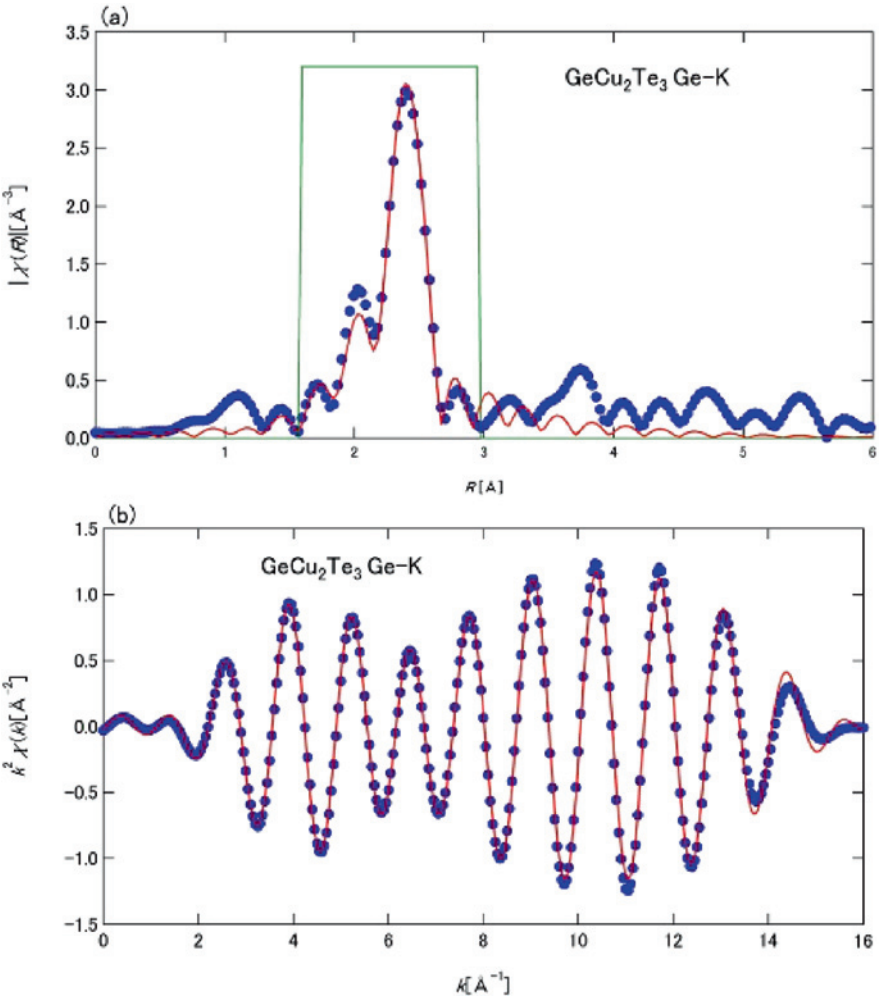

Figure 5: Comparison of experimental data near the Ge K absorption edge in $GeCu_2Te_3$ XAFS datasets (circles) with the analyzed curves (solid lines) obtained by fitting. (a) The Fourier transforms of the XAFS oscillations and (b) its inverse-Fourier transform. A thin straight line is window function.

The obtained Debye–Waller factors for the Ge–Te correlations are larger than those of Cu–Te by about 0.0005 $Å^2$, indicating that the Ge–Te bond lengths are slightly more fluctuated than the Cu–Te bond lengths.

Table 2 shows the comparison between the averaged nearest neighbor distances obtained by XRD and XAFS measurements, together with the values in amorphous $GeCu_2Te_3$ obtained by XAFS measurements [7]. The averaged Ge–Te

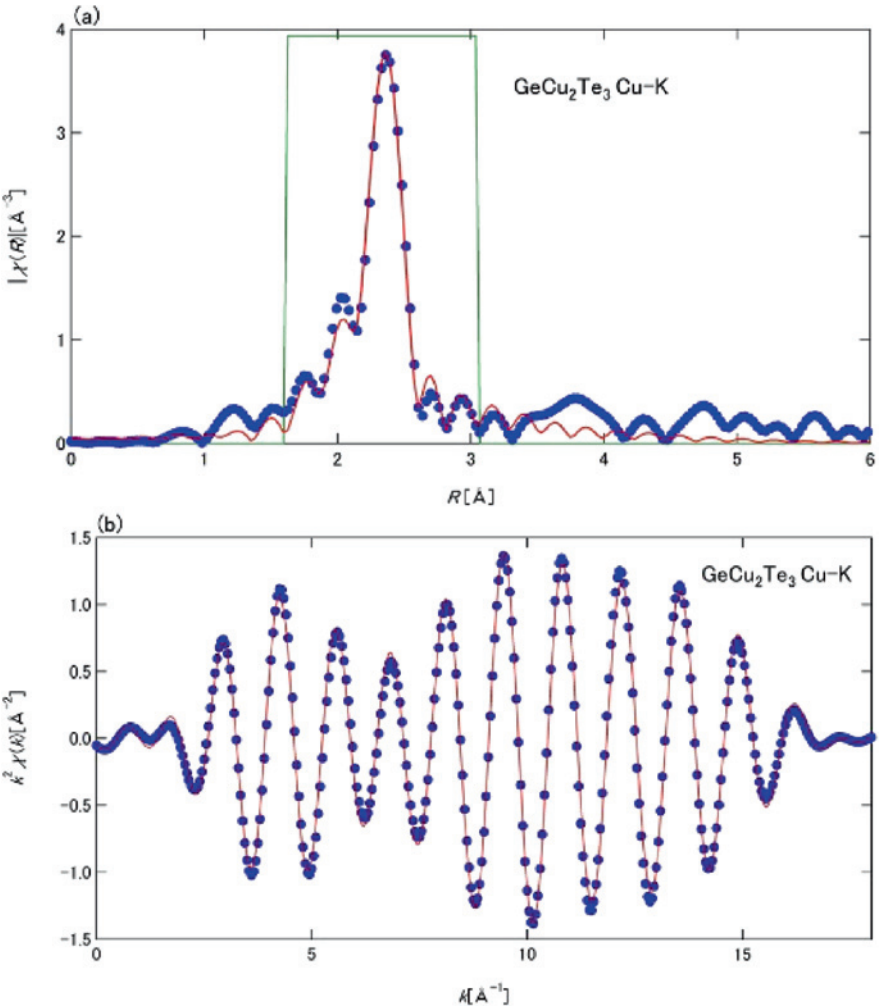

Figure 6: Comparison of experimental data near the Cu K absorption edge in $GeCu_2Te_3$ XAFS datasets (circles) with the analyzed curves (solid lines) obtained by fitting. (a) The Fourier transforms of the XAFS oscillations and (b) its inverse-Fourier transform. A thin straight line is window function.

and Cu–Te interatomic distances in crystal $GeCu_2Te_3$ obtained by XRD are 2.51 ± 0.01 and 2.61 ± 0.01 Å [3], respectively. On the contrary, the averaged Ge–Te and Cu–Te interatomic distances in crystal $GeCu_2Te_3$ obtained by the present XAFS measurements are 2.60 ± 0.01 and 2.54 ± 0.01 Å, respectively.

Table 1: R_j and σ_i^2 in crystal $GeCu_2Te_3$ determined by XAFS measurements with fixed N_j.

	N_j	R_j [Å]	σ_i^2 [Å^2]
Ge–Te1	2	2.585	0.00258
Ge–Te2	2	2.617	0.00261
Cu–Te1	2	2.537	0.00212
Cu–Te2	1	2.574	0.00215
Cu–Te3	1	2.531	0.00211

Table 2: Comparison of the averaged R_j in crystal $GeCu_2Te_3$ between the XRD [3] and XAFS measurements together with the averaged R_j in amorphous $GeCu_2Te_3$ obtained by XAFS measurements [7].

	XRD crystal averaged [3]	XAFS crystal averaged	XAFS amorphous [7]
Ge–Te	2.51 (1)	2.60 (1)	2.61 (2)
Cu–Te	2.61 (1)	2.54 (1)	2.55 (3)

Of particular interest is that the Ge–Te distances in crystal $GeCu_2Te_3$ obtained by the present XAFS measurements are larger than those obtained by XRD, and the Cu–Te distances in crystal $GeCu_2Te_3$ obtained by XAFS are smaller than those by XRD.

Why does such a discrepancy between the XRD and XAFS results occur even for the interatomic distances in the crystal? Fons et al. suggested that XRD is only sensitive to the average structure and insensitive to the local distortions [8]. Namely, XRD measures averaged periodicity of the electron distributions, and it is impossible to determine the exact positions of atoms, and the actual atoms are not guaranteed to be located at the lattice positions obtained by XRD. On the other hand, XAFS measurements are able to directly determine local atomic positions around the central atom [8].

We explain the differences between the long-range periodicity and local structure for the Cu–Te bond using a schematic view of Figure 7. If Cu and Te atoms have the position fluctuations, the average positions are located at the centers, and are observed by XRD. However, it is possible that the individual Cu–Te bond lengths are much shorter, and detected by XAFS. In the Ge–Te case, the opposite situations can occur. For this reason, XAFS measurements correctly determine the local interatomic distances rather than XRD.

The structure of amorphous $GeCu_2Te_3$ has been investigated by using experimental results of XRD and XAFS measurements, and reverse Monte Carlo

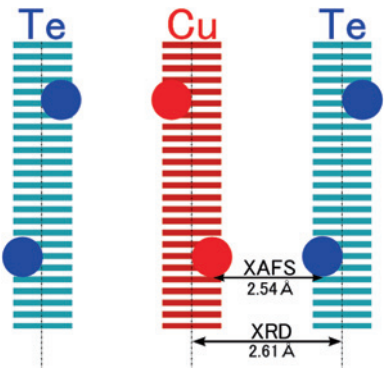

Figure 7: Schematic illustration of the difference between XRD and XAFS measurements.

(RMC) simulation [7]. The average coordination numbers around Ge, Cu, and Te are close to four as in the crystal phase. The Ge–Te and Cu–Te distances in amorphous $GeCu_2Te_3$ obtained by XAFS measurements are 2.61 ± 0.02 and 2.55 ± 0.03 Å, respectively [7]. It is very interesting that the averaged Ge–Te and Cu–Te distances in crystal $GeCu_2Te_3$ obtained by the present XAFS measurements are mostly equal to those in amorphous $GeCu_2Te_3$ [7] as shown in Table 2.

Therefore, both the crystalline and amorphous $GeCu_2Te_3$ seem to be built up of closely similar $GeTe_4$ and $CuTe_4$ tetrahedrons. Namely, the local atomic arrangements in $GeCu_2Te_3$ are almost preserved upon the crystalline-amorphous phase change. This would be the reason why the phase change of $GeCu_2Te_3$ rapidly occurs in about several 10 ns.

4 Conclusion

The local structure of crystalline $GeCu_2Te_3$ was investigated by XAFS measurements around the Ge and Cu K absorption edges. A discrepancy was found in the Ge–Te and Cu–Te interatomic distances, i.e., the Ge–Te distances obtained by XAFS are larger than those by XRD, and the Cu–Te distances are smaller than those by XRD. Furthermore, the averaged Ge–Te and Cu–Te distances obtained by the present XAFS measurements are mostly equal to those in amorphous $GeCu_2Te_3$. Therefore, both the crystalline and amorphous $GeCu_2Te_3$ seem to be built up of closely similar $GeTe_4$ and $CuTe_4$ tetrahedrons. As a result, the phase change of $GeCu_2Te_3$ occurs without large changes in the local atomic arrangements. This would be the reason why the phase change of $GeCu_2Te_3$ rapidly occurs in about several 10 ns.

Acknowledgement: The XAFS experiments were carried out at the XAFS beamline BL12C of PF-KEK (Proposal No. 2010G559 and 2012G522). We thank Prof. F. Ichikawa for the support of XRD measurements.

References

1. T. Kamada, Y. Sutou, M. Sumiya, Y. Saito, and J. Koike, Thin Solid Films **520** (2012) 4389.
2. Y. Sutou, T. Kamada, M. Sumiya, Y. Saito, and J. Koike, Acta Mater. **60** (2012) 872.
3. G. E. Delgado, A. J. Mora, M. Pirela, A. Velásquez-Velásquez, M. Villarreal, and B. J. Fernández, Phys. Status Solidi A **201** (2004) 2900.
4. B. B. Shama, R. Ayyar, and H. Singh, Phys. Status Solidi A **40** (1977) 691.
5. B. Ravel and M. Newville, J. Synchrotron Radiat. **12** (2005) 537.
6. M. Newville, J. Synchrotron Radiat. **8** (2001) 96.
7. P. Jóvári, Y. Sutou, I. Kaban, Y. Saito, and J. Koike, Scripta Mater. **68** (2013) 122.
8. P. Fons, A. V. Kolobov, M. Krbal, J. Tominaga, K. S. Andrikopoulos, S. N. Yannopoulos, G. A. Voyiantzis, and T. Uruga, Phys. Rev. B **82** (2010) 155209-1.